Dynamically Disordered Quantum Walk as a Maximal Entanglement Generator

Rafael Vieira,[1] Edgard P. M. Amorim,[1,*] and Gustavo Rigolin[2,†]

[1]*Departamento de Física, Universidade do Estado de Santa Catarina, 89219-710 Joinville, Santa Catarina, Brazil*
[2]*Departamento de Física, Universidade Federal de São Carlos, 13565-905 São Carlos, São Paulo, Brazil*

(Received 14 May 2013; revised manuscript received 21 June 2013; published 31 October 2013)

We show that the entanglement between the internal (spin) and external (position) degrees of freedom of a qubit in a random (dynamically disordered) one-dimensional discrete time quantum random walk (QRW) achieves its maximal possible value asymptotically in the number of steps, outperforming the entanglement attained by using ordered QRW. The disorder is modeled by introducing an extra random aspect to QRW, a classical coin that randomly dictates which quantum coin drives the system's time evolution. We also show that maximal entanglement is achieved independently of the initial state of the walker, study the number of steps the system must move to be within a small fixed neighborhood of its asymptotic limit, and propose two experiments where these ideas can be tested.

DOI: 10.1103/PhysRevLett.111.180503 PACS numbers: 03.67.Bg, 03.65.Ud, 03.67.Ac, 05.40.Fb

Imagine we have a qubit, a quantum particle that in addition to its external degrees of freedom (position and momentum) has a spin-1/2-like internal one (two-level system) [1]. We assume it evolves in time as follows. We first apply a unitary operation C (our ''quantum coin'') acting only on the qubit's internal degree of freedom, leaving it generally in a superposition of spin up and down. We then apply another unitary operation S that correlates the displacement of the qubit to its internal degree of freedom. It moves right if the spin state at a given site is up and left otherwise. In this way, we entangle the internal and external degrees of freedom of the system. Successive applications of the previous procedure lead to the discrete time evolution (displacement) of the qubit. This is what we call the one-dimensional discrete time quantum random walk (QRW) [2,3].

The key difference between the classical random walk (CRW) [4] and QRW is the superposition principle of quantum mechanics, a feature that is obviously lacking in CRW. The application of C followed by the displacement operator S at each step generates a catlike state among all possible positions of the particle, setting the stage for interference effects to take place. The interference among the probability amplitudes manifests itself by producing a position probability distribution $P(j)$ drastically different from the classical one. Indeed, $P(j)$ for the unbiased CRW is always peaked about the initial position and drops off exponentially with the square of the distance (Gaussian distribution). Also, its variance σ^2 is proportional to the number n of steps (coins flipped). This is the diffusive behavior. For the unbiased QRW, however, $P(j)$ is roughly uniform as we move away from the origin, having peaks far from it. Moreover, depending on the initial spin state, we can have one peak at the left, or at the right, or two symmetrical peaks [3], and $\sigma^2 \propto n^2$, a quadratic gain (ballistic behavior) in the propagation of the particle when compared to CRW. Furthermore, due to the $SU(2)$ structure of C, we have a coin with three independent parameters, while classically there is only one.

Both CRW and QRW, in the one- or higher-dimensional versions, have many important applications [5]. And the majority of studies dealing with QRW assume that C is the same during all steps of the walk or changes in a deterministic way [3,8–13]. What would happen, though, if noise, disorder, or fluctuations change C from one step to the other? What would happen if C changes randomly between two possible coins? A naive guess would suggest that *all* features of QRW may be washed out by such a process. Indeed, it is known that *some* typical features of QRW, such as $P(j)$ and σ^2, change in such random processes and approach the classical case [14]. However, so far no systematic numerical and/or analytical studies along this line were done for the entanglement content of the walker and for any initial condition. The only exception is Ref. [15], which came to our knowledge after finishing this work and where for only one initial condition and a particular type of static and dynamical disorder the behavior of entanglement was numerically investigated for a 100-step walk.

Our main goal here is to investigate such an extra random aspect on a QRW and analyze whether or not it is detrimental to its entanglement generation capacity. Our main finding is, surprisingly, that the opposite from the naive guess occurs when it comes to entanglement generation using a dynamically disordered QRW. We show that the entanglement, a genuine quantum feature, between the internal and external degrees of freedom of the walker is enhanced when C changes from one step to the other in a truly random way. We also show that we achieve, asymptotically in the number of steps, a maximally entangled state. Moreover, we show that this effect is independent of the initial condition, contrary to standard entanglement generation schemes that rely critically on the initial state of the system and never achieve maximal entanglement [12]. It is worth mentioning that this initial state

independence that we show here has important practical consequences and shows that the entanglement generation scheme here presented is robust against imperfections in the preparation of the initial state.

In order to explore these ideas, we introduce a walker that combines the features of both the classical and quantum ones in a single formalism. It has two random ingredients, one of which is a classical coin similar to that of CRW. This coin dictates which quantum coin (the source of position randomness) will be used at each step of the walk. This is the essence of this walker, and the presence of these two different random aspects, one classical and another quantum, leads us to call it a random quantum random walk (RQRW) process. We show in Ref. [16] that CRW and QRW are two particular cases of RQRW. Note that the quantum random aspect manifests itself only when we measure the position or spin of the walker (measurement postulate of quantum mechanics). The dynamics is unitary, however, leading some authors to call the ordered case simply QW instead of QRW.

Mathematical formalism.—The Hilbert space of RQRW is $\mathcal{H} = \mathcal{H}_C \otimes \mathcal{H}_P$, where $\mathcal{H}_C$ is a two-dimensional complex vector space associated to the spin states $\{|\uparrow\rangle, |\downarrow\rangle\}$ and $\mathcal{H}_P$ is an infinite-dimensional but countable complex Hilbert space spanned by all integers. Its base is represented by the kets $|j\rangle$, $j \in \mathbb{Z}$, and they denote the position of the qubit on the lattice. With this notation we write an arbitrary initial state of the qubit (walker) as $|\Psi(0)\rangle = \sum_j [a(j,0)|\uparrow\rangle \otimes |j\rangle + b(j,0)|\downarrow\rangle \otimes |j\rangle]$, with $\sum_j [|a(j,0)|^2 + |b(j,0)|^2] = 1$ being the normalization condition and j running over all integers. The time t is discrete, and it denotes the steps of the walker. In an n-step process, the time changes from $t = 0$ to $t = n$ in increments of one, and the walker's state is $|\Psi(n)\rangle = U(n)\ldots U(1)|\Psi(0)\rangle = \mathcal{T}\prod_{t=1}^{n} U(t)|\Psi(0)\rangle$, where $\mathcal{T}$ denotes a time-ordered product and

$$U(t) = S[C(t) \otimes \mathbb{1}_P]. \tag{1}$$

Here $\mathbb{1}_P$ is the identity operator acting on the space $\mathcal{H}_P$, $C(t)$ the time-dependent quantum coin, and S the conditional displacement operator. The operator S moves the qubit at site j to the site $j+1$ if its spin is up and to the site $j-1$ if its spin is down. By using the present notation, $S = \sum_j (|\uparrow\rangle\langle\uparrow| \otimes |j+1\rangle\langle j| + |\downarrow\rangle\langle\downarrow| \otimes |j-1\rangle\langle j|)$.

An arbitrary $C(t)$ is given by the most general way of writing an $SU(2)$ unitary transformation. Up to an irrelevant global phase we have $C(t) = c_{\uparrow\uparrow}(t)|\uparrow\rangle\langle\uparrow| + c_{\uparrow\downarrow}(t)|\uparrow\rangle\times\langle\downarrow| + c_{\downarrow\uparrow}(t)|\downarrow\rangle\langle\uparrow| + c_{\downarrow\downarrow}(t)|\downarrow\rangle\langle\downarrow|$, with $c_{\uparrow\uparrow}(t) = \sqrt{q(t)}$, $c_{\uparrow\downarrow}(t) = \sqrt{1-q(t)}e^{i\theta(t)}$, $c_{\downarrow\uparrow}(t) = \sqrt{1-q(t)}e^{i\varphi(t)}$, and $c_{\downarrow\downarrow}(t) = -\sqrt{q(t)}e^{i[\theta(t)+\varphi(t)]}$. Here $0 \le q(t) \le 1$ and $0 \le \theta(t), \varphi(t) \le 2\pi$. The first parameter controls the bias of $C(t)$. For $q(t) = 1/2$ the coin creates an equal superposition of the spin states when acting on either $|\uparrow\rangle$ or $|\downarrow\rangle$ and an unbalanced one for $q(t) \neq 1/2$. The last two parameters control the relative phase between the two states in the superposition. Note that we are exploring the full $SU(2)$ structure of $C(t)$ with its three independent parameters, which makes it more general than the ones in Ref. [14]. Time-dependent walkers were also explored in [17], where, instead of C, S was made time dependent, and in [18,19].

The general time evolution can be obtained by applying $U(t)$ [Eq. (1)] to an arbitrary state at time $t-1$. This leads to $|\Psi(t)\rangle = U(t)|\Psi(t-1)\rangle = \sum_j [a(j,t)|\uparrow\rangle|j\rangle + b(j,t)|\downarrow\rangle|j\rangle]$, where

$$\begin{aligned} a(j,t) &= c_{\uparrow\uparrow}(t)a(j-1,t-1) + c_{\uparrow\downarrow}(t)b(j-1,t-1), \\ b(j,t) &= c_{\downarrow\uparrow}(t)a(j+1,t-1) + c_{\downarrow\downarrow}(t)b(j+1,t-1). \end{aligned} \tag{2}$$

We will focus here on two types of RQRW (see Fig. 1). The first one deals with only two quantum coins: C_1 and C_2. At each step of the walk, the decision to use C_1 or C_2 is made by the result of a classical coin. If we get heads at step t, we use C_1, and if we get tails, we use C_2. We call this process a RQRW_2, with the subindex denoting that our choices are made randomly between two quantum coins.

In the second RQRW we have an infinite number of $C(t)$ to choose at each step. The independent parameters of $C(t)$, namely, $q(t)$, $\theta(t)$, and $\varphi(t)$, are chosen from continuous uniform distributions spanning the range of their allowed values. Note that we can have a walk where either one, two, or all parameters change at each step. We call such walks RQRW_∞.

Entanglement.—Since $\rho(t) = |\Psi(t)\rangle\langle\Psi(t)|$ is pure, we quantify the entanglement between the internal and external degrees of freedom by the von Neumann entropy of the partially reduced state $\rho_C(t) = \mathrm{Tr}_P[\rho(t)]$ [20], $S_E[\rho(t)] = -\mathrm{Tr}[\rho_C(t)\log_2\rho_C(t)]$, with $\mathrm{Tr}_P(\cdot)$ being the trace over the position degrees of freedom. S_E is 0 for separable states and 1 for maximally entangled ones. Since $\rho_C(t) = \alpha(t)|\uparrow\rangle\langle\uparrow| + \beta(t)|\downarrow\rangle\langle\downarrow| + \gamma(t)|\uparrow\rangle\langle\downarrow| + \gamma^*(t)|\downarrow\rangle\langle\uparrow|$, where $\alpha(t) = \sum_j |a(j,t)|^2$, $\beta(t) = \sum_j |b(j,t)|^2$, $\gamma(t) = \sum_j a(j,t)\times b^*(j,t)$, and z^* is the complex conjugate of z, we have

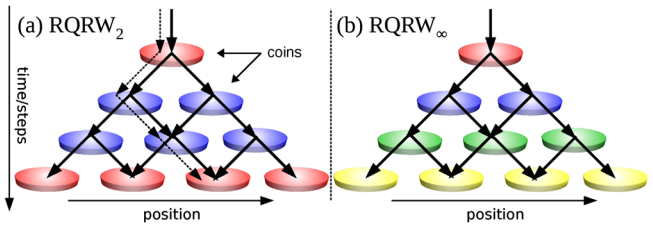

FIG. 1 (color online). (a) The dashed line represents a possible realization of CRW, where no superposition occurs. The solid curves represent probability amplitudes for RQRW_2, where only two $C(t)$ are allowed (red and blue disks). (b) Schematic view for RQRW_∞, where $C(t)$ are chosen randomly from uniform continuous distributions of quantum coins (at each step a different color or coin is used). Note that at each step all coins or colors are the same (dynamical disorder).

$S_E[\rho(t)] = -\lambda_+(t)\log_2\lambda_+(t) - \lambda_-(t)\log_2\lambda_-(t)$, with $\lambda_\pm = \{1/2 \pm \sqrt{1/4 - \alpha(t)[1-\alpha(t)] + |\gamma(t)|^2}\}$ being the eigenvalues of $\rho_C(t)$.

Results.—We start by studying two typical representatives of RQRW. The first one is RQRW_2 with C_1 being the Hadamard (H) coin [$q(t) = 1/2$, $\theta(t) = \varphi(t) = 0$] and C_2 the Fourier or Kempe (F) coin [$q(t) = 1/2$, $\theta(t) = \varphi(t) = \pi/2$]. Note that the latter coin introduces a $\pi/2$ relative phase between $|\uparrow\rangle$ and $|\downarrow\rangle$. The other walk is RQRW_∞, where at each step the values of $q(t)$, $\theta(t)$, and $\varphi(t)$ are chosen randomly from three distinct continuous uniform distributions.

In order to investigate the dependence of the asymptotic behavior of S_E on initial conditions, we run several thousand numerical experiments, each with a different initial condition. Each realization of the walk gives at step t a value for S_E, and in Fig. 2 we show the average values of S_E over all realizations at each step t.

As can be seen from Fig. 2, the average entanglement $\langle S_E\rangle$ approaches the maximal value possible ($S_E = 1$) for both RQRW cases after a few hundred steps. For comparison, we show the usual QRW with a Hadamard coin, where clearly $\langle S_E\rangle \neq 1$ asymptotically. Indeed, for the ordered case the asymptotic value of S_E is highly sensitive to the initial conditions, and the set of initial states giving high values of S_E is not dense. An important example is the Hadamard walk, where it can be shown [12] that the asymptotic values of S_E continuously oscillate between $S_E = 0.661$ and $S_E = 0.979$ as we cover a set of initial conditions similar to the ones in Fig. 2.

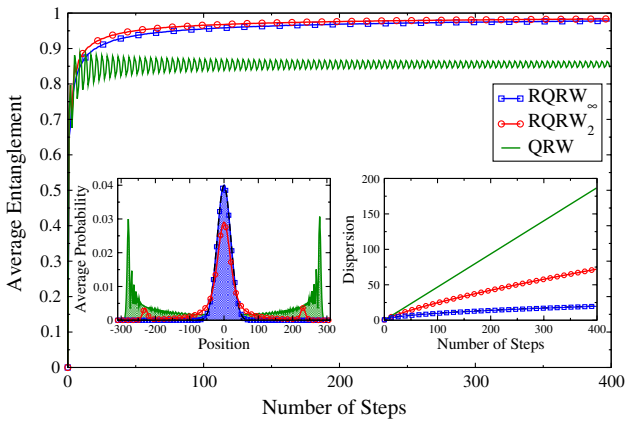

FIG. 2 (color online). $\langle S_E\rangle$ was computed by averaging over 16 384 initial conditions of the form $|\Psi(0)\rangle = (\cos\alpha_s|\uparrow\rangle + e^{i\beta_s}\sin\alpha_s|\downarrow\rangle)\otimes(\cos\alpha_p|-1\rangle + e^{i\beta_p}\sin\alpha_p|1\rangle)$, with $\alpha_{s,p} \in [0, \pi]$ and $\beta_{s,p} \in [0, 2\pi]$. The first realization used the initial condition $(\alpha_s, \beta_s, \alpha_p, \beta_p) = (0, 0, 0, 0)$ and the subsequent ones all quadruples of points in independent increments of 0.4 until $\alpha_{s,p} = \pi$ and $\beta_{s,p} = 2\pi$. We worked with a 400-step walk. The blue (square) curve gives RQRW_∞, the red (circle) one RQRW_2, and the green (solid) one the Hadamard QRW. The left inset shows the average position probability distributions [$\langle P(j)\rangle$] after 400 steps and the right one the average dispersions ($\langle\sqrt{\sigma^2}\rangle$). The black dashed curves represent the expected results for CRW starting at the origin, and they overlap with the curves for RQRW_∞, which is more localized than RQRW_2. The two spikes on $\langle P(j)\rangle$ for RQRW_2 are due to the fact that it is built on the Hadamard and Fourier coins, where these spikes are a common trend.

To gain further insights into the asymptotic limit of S_E, we run another set of numerical experiments for the three walks described in Fig. 2, but now going up to 1000 steps and also counting the number of initial conditions leading to high values of S_E. By looking at Fig. 3, it is clear that $S_E \to 1$ for RQRW_∞ and RQRW_2, while the Hadamard QRW asymptotic entanglement is highly sensitive to the initial conditions.

Now, since S_E is bounded from above by one, $\langle S_E\rangle \to 1$ implies that for RQRW the set of initial states in which $S_E \to 1$ asymptotically is dense. In other words, this suggests that in the asymptotic limit $S_E \to 1$ for any initial condition. The justification of the last assertion is given by the following theorem.

Theorem.—In the asymptotic limit and for any initial condition, $S_E \to 1$ if the quantum coin acting on the walker at each step is a random $SU(2)$ unitary operator.

Here we outline the main ideas leading to the proof, and the details are given in [16]. In the long time regime, $\rho_C(t+1) = \rho_C(t) + \mathcal{O}(t^{-1/4})$. Thus, $\rho_C(t+1) = \rho_C(t)$ for $t \to \infty$. In terms of its coefficients, $\alpha(t+1) = \alpha(t)$ and $\gamma(t+1) = \gamma(t)$. This, plus the time evolution of $\alpha(t)$ and $\gamma(t)$, that can be computed with Eq. (2), leads to $\mathrm{Re}\{[c_{\uparrow\uparrow}(t+2)/c_{\uparrow\downarrow}(t+2) - c_{\uparrow\uparrow}(t+1)/c_{\uparrow\downarrow}(t+1)]\gamma(t)\} = 0$. Note that, for constant coins, this equality is trivially

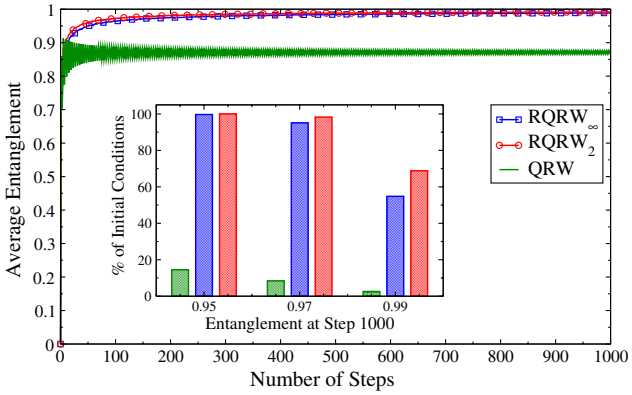

FIG. 3 (color online). $\langle S_E\rangle$ was obtained by averaging over 2016 localized initial conditions given as $|\Psi(0)\rangle = (\cos\alpha_s|\uparrow\rangle + e^{i\beta_s}\sin\alpha_s|\downarrow\rangle)\otimes|0\rangle$, where $\alpha_s \in [0, \pi]$ and $\beta_s \in [0, 2\pi]$. The first realization used the initial condition $(\alpha_s, \beta_s) = (0, 0)$ and the next ones all pairs of points in independent increments of 0.1 until $\alpha_s = \pi$ and $\beta_s = 2\pi$. We worked with a 1000-step walk. The inset shows the rate of initial conditions leading to S_E greater than 0.95, 0.97, and 0.99 at step 1000. Note that for RQRW [middle (blue) and right (red) bars] almost 100% of the initial conditions lead to $S_E > 0.97$, while for QRW [left (green) bar] this occurs for less than 10%.

satisfied. But for time-dependent random ones, the term inside the brackets is a random complex number $z(t) = x(t) + iy(t)$, with $x(t)$ and $y(t)$ random reals. Hence $x(t)\mathrm{Re}[\gamma(t)] - y(t)\mathrm{Im}[\gamma(t)] = 0$. Repeating this argument for a subsequent time leads to $x(t+1)\mathrm{Re}[\gamma(t)] - y(t+1)\mathrm{Im}[\gamma(t)] = 0$. These expressions form a homogeneous system of linear equations on the variables $\mathrm{Re}[\gamma(t)]$ and $\mathrm{Im}[\gamma(t)]$. A nontrivial solution exists if the determinant of its coefficients is zero. But this will almost surely not happen, since $x(t)$, $y(t)$, $x(t+1)$, and $y(t+1)$ are four independent random numbers. Thus $\gamma(t) = 0$ and $\alpha(t) = 1/2$, since the dynamics and the asymptotic condition give $\alpha(t) = 1/2 + \mathrm{Re}[\gamma(t)c_{\uparrow\uparrow}(t+1)/c_{\uparrow\downarrow}(t+1)]$. These values for $\gamma(t)$ and $\alpha(t)$ give $S_E = 1$, a maximally entangled state.

In Ref. [16], we investigate numerically other RQRW, some of them not covered by the theorem, and how much disorder we must have to achieve $S_E \to 1$ asymptotically. We show that weak disorder is sufficient to generate highly entangled states for arbitrary initial conditions in a variety of RQRW and give further details about the probability distribution of the walker and its dispersion properties. Finally, we also investigate how fast highly nonlocal initial conditions (Gaussian distributions) approach the asymptotic limit $S_E \to 1$.

Experimental implementation.—Current technology allows one to implement in at least two ways the previous walks. The first one is based on passive optical elements, such as quarter (QWP) and half (HWP) wave plates and polarizing beam splitters (PBSs), plus a fast-switching electro-optical modulator (EOM) [21], where the internal degree of freedom of the walker is the polarization of a photon and the position or external one is mapped to different arrival times of the photon at the photodetector (time bins) [22].

The second way also uses photons as walkers, but it is based on integrated photonics, where a disordered walk is built on integrated waveguide circuits, providing perfect phase stability. By using state-of-the-art femtosecond laser writing techniques, the authors in Ref. [23] were able to wrought an array of interferometers in a glass that reproduces the dynamics of RQRW [24].

To test the ideas here presented, we need to measure the entanglement of the walker, which is obtained if we know the coin state $\rho_C(t)$. But $\rho_C(t)$ is determined by slightly changing the two schemes outlined above. Indeed, since a general photon polarization state is written as $\rho_C(t) = \mathbb{1}_C + \sum_{j=1}^{3} r_j \sigma_j$, with σ_j being Pauli matrices, we can determine $\rho_C(t)$ if we measure r_j. But this is achieved by measuring the average polarization of the photon in the vertical (horizontal) axis (r_3), in the $\pm 45°$ axis (r_1), and the average right (left) circular polarization (r_2) [25]. These measurements can be easily implemented by properly arranging a HWP and QWP before the photon passes a PBS with photodetectors at each one of its arms. Note that the raw data are related to $\rho(t)$, and we need to trace out its position degrees of freedom (postprocessing measurement) to get $\rho_C(t)$. In Ref. [16], we show that just a few steps are enough to have different predictions for the behavior of S_E if we work with either RQRW_2 or QRW.

Summary.—We defined the RQRW, a discrete time quantum random walk scheme whose unitary evolution at each step is chosen randomly by using a two-sided (or infinitely sided) classical coin. We showed that both the usual classical and quantum random walks are particular cases of RQRW. We then studied its entanglement generation capacity. We showed that RQRW creates maximally entangled sates in the asymptotic limit for several types of dynamical disorder (random time evolution), contrary to the ordered QRW. Furthermore, and surprisingly, we proved that RQRW entanglement creation capabilities are independent of the initial condition of the walker, another property in contrast to ordered QRW.

Finally, we point out that our findings naturally lead to new important questions. For example, what is the interplay between order or disorder and entanglement creation for two- or three-dimensional walkers? What would happen to the entanglement for static disorder [15,21,23]? Can the previous results be adapted to the case of two or more [13] walkers to improve the creation of bipartite and multipartite entanglement, respectively, only among the internal degrees of freedom? We believe investigations along these lines may bring other unexpected and intriguing results and foster the development of new entanglement generation protocols.

The authors thank the anonymous referee for many insightful suggestions that improved the presentation of this manuscript. R. V. thanks CAPES (Brazilian Agency for the Improvement of Personnel of Higher Education) for funding. G. R. thanks the Brazilian agencies CNPq (National Council for Scientific and Technological Development) and FAPESP (State of São Paulo Research Foundation) for funding and CNPq/FAPESP for financial support through the National Institute of Science and Technology for Quantum Information.

*eamorim@joinville.udesc.br
†rigolin@ufscar.br

[1] This internal degree of freedom can be the spin of an electron, the polarization of photons, or the ground and excited states of an atom.
[2] Y. Aharonov, L. Davidovich, and N. Zagury, Phys. Rev. A **48**, 1687 (1993).
[3] J. Kempe, Contemp. Phys. **44**, 307 (2003); S. E. Venegas-Andraca, Quantum Inf. Process. **11**, 1015 (2012).
[4] K. Pearson, Nature (London) **72**, 294 (1905); **72**, 342 (1905); L. Rayleigh, *ibid.* **72**, 318 (1905).
[5] CRW is employed from the modeling of biological processes [6] to polymer physics [7]. QRW has proved to give important insights into the implementation of quantum search algorithms [8], the understanding of the physics of

photosynthesis [9], the construction of a universal quantum computer [10,11], and the generation of entangled states for systems with one [12] and more walkers [13].

[6] H. C. Berg, *Random Walks in Biology* (Princeton University, Princeton, NJ, 1993).

[7] P.-G. de Gennes, *Scaling Concepts in Polymer Physics* (Cornell University, Ithaca, 1979).

[8] N. Shenvi, J. Kempe, and K. Birgitta Whaley, Phys. Rev. A **67**, 052307 (2003).

[9] G. S. Engel, T. R. Calhoun, E. L. Read, T.-Kyu Ahn, T. Mančal, Y.-C. Cheng, R. E. Blankenship, and G. R. Fleming, Nature (London) **446**, 782 (2007).

[10] A. M. Childs, Phys. Rev. Lett. **102**, 180501 (2009).

[11] N. B. Lovett, S. Cooper, M. Everitt, M. Trevers, and V. Kendon, Phys. Rev. A **81**, 042330 (2010).

[12] I. Carneiro, M. Loo, X. Xu, M. Girerd, V. Kendon, and P. L. Knight, New J. Phys. **7**, 156 (2005); G. Abal, R. Siri, A. Romanelli, and R. Donangelo, Phys. Rev. A **73**, 042302 (2006); S. Salimi and R. Yosefjani, Int. J. Mod. Phys. B **26**, 1250112 (2012).

[13] S. E. Venegas-Andraca and S. Bose, arXiv:0901.3946; S. K. Goyal and C. M. Chandrashekar, J. Phys. A **43**, 235303 (2010); C. Di Franco, M. Mc Gettrick, and Th. Busch, Phys. Rev. Lett. **106**, 080502 (2011); B. Allés, S. Gündüç, and Y. Gündüç, Quantum Inf. Process. **11**, 211 (2012); E. Roldán, C. DiFranco, F. Silva, and G. J. de Valcárcel, Phys. Rev. A **87**, 022336 (2013); S. Moulieras, M. Lewenstein, and G. Puentes, J. Phys. B **46**, 104005 (2013).

[14] P. Ribeiro, P. Milman, and R. Mosseri, Phys. Rev. Lett. **93**, 190503 (2004); M. C. Bañuls, C. Navarrete, A. Pérez, E. Roldán, and J. C. Soriano, Phys. Rev. A **73**, 062304 (2006).

[15] C. M. Chandrashekar, arXiv:1212.5984.

[16] See Supplemental Material at http://link.aps.org/supplemental/10.1103/PhysRevLett.111.180503 for a proof that CRW and QRW are particular cases of RQRW, a detailed proof of the theorem in the main text, numerical studies of several other RQRW, and a detailed description of how to experimentally test these ideas with current technology.

[17] O. Buerschaper and K. Burnett, arXiv:quant-ph/0406039; A. Wójcik, T. Łuczak, P. Kurzyński, A. Grudka, and M. Bednarska, Phys. Rev. Lett. **93**, 180601 (2004); A. Romanelli, A. Auyuanet, R. Siri, G. Abal, and R. Donangelo, Physica (Amsterdam) **352A**, 409 (2005).

[18] D. Shapira, O. Biham, A. J. Bracken, and M. Hackett, Phys. Rev. A **68**, 062315 (2003); A. Joye, Commun. Math. Phys. **307**, 65 (2011).

[19] A. Ahlbrecht, C. Cedzich, R. Matjeschk, V. B. Scholz, A. H. Werner, and R. F. Werner, Quantum Inf. Process. **11**, 1219 (2012); A. Ahlbrecht, H. Vogts, A. H. Werner, and R. F. Werner, J. Math. Phys. (N.Y.) **52**, 042201 (2011); A. Ahlbrecht, V. B. Scholz, and A. H. Werner, J. Math. Phys. (N.Y.) **52**, 102201 (2011).

[20] C. H. Bennett, H. J. Bernstein, S. Popescu, and B. Schumacher, Phys. Rev. A **53**, 2046 (1996).

[21] A. Schreiber, K. N. Cassemiro, V. Potoček, A. Gábris, I. Jex, and Ch. Silberhorn, Phys. Rev. Lett. **106**, 180403 (2011); A. Schreiber, K. N. Cassemiro, V. Potoček, A. Gábris, P. J. Mosley, E. Andersson, I. Jex, and Ch. Silberhorn, Phys. Rev. Lett. **104**, 050502 (2010).

[22] The random coin operator C is implemented by using HWP and EOM, while the conditional displacement operator S two PBSs and a fiber delay line where one polarization follows a longer optical path. Also, arbitrary initial conditions are simply generated by QWP and HWP. An important feature of the scheme in Ref. [21] is its scalability with the number of steps. Indeed, the techniques of optical feedback loop allow the implementation of a many-step walk using few optical elements. In Ref. [21], the authors have already implemented 28-step walks with static and dynamical disorder.

[23] A. Crespi, R. Osellame, R. Ramponi, V. Giovannetti, R. Fazio, L. Sansoni, F. De Nicola, F. Sciarrino, and P. Mataloni, Nat. Photonics **7**, 322 (2013).

[24] In integrated waveguide circuits, the PBS is a directional coupler and phase shifts are implemented by writing circuits with different length or deformation.

[25] A. Peres, *Quantum Theory: Concepts and Methods* (Kluwer Academic, New York, 2002).